Received: 13 January 2018 | Revised: 25 May 2018 | Accepted: 11 June 2018

DOI: 10.1111/odi.12915

ORIGINAL ARTICLE

WILEY ORAL DISEASES

A novel *PTCH1* mutation underlies nonsyndromic cleft lip and/or palate in a Han Chinese family

Huaxiang Zhao[1]* | Wenjie Zhong[1]* | Chuntao Leng[2] | Jieni Zhang[1] | Mengqi Zhang[1] | Wenbin Huang[1] | Yunfan Zhang[1] | Weiran Li[1] | Peizeng Jia[1] | Jiuxiang Lin[1] | Gulibaha Maimaitili[2] | Feng Chen[3]

[1]Department of Orthodontics, Peking University School and Hospital of Stomatology, Beijing, China

[2]Department of Stomatology, The Fifth Affiliated Hospital of Xinjiang Medical University, Urumqi, China

[3]Central Laboratory, Peking University School and Hospital of Stomatology, Beijing, China

Correspondence
Gulibaha Maimaitili, Department of Stomatology, The Fifth Affiliated Hospital of Xinjiang Medical University, Urumqi, China.
Email: gulibaha_1972@163.com
and
Feng Chen, Central Laboratory, Peking University School and Hospital of Stomatology, 22 Zhongguancun South Avenue, Haidian District, 100081, Beijing, China.
Email: moleculecf@gmail.com

Funding information
Interdisciplinary Medicine Seed Fund of Peking University, Grant/Award Number: BMU2017 MB006; Beijing Municipal Natural Science Foundation, Grant/Award Number: 7182184

Abstract

Objectives: Cleft lip and/or palate (CL/P) is the most common craniofacial congenital disease, and it has a complex aetiology. This study aimed to identify the causative gene mutation of a Han Chinese family with CL/P.

Subjects and Methods: Whole exome sequencing was conducted on the proband and her mother, who exhibited the same phenotype. A Mendelian dominant inheritance model, allele frequency, mutation regions, functional prediction and literature review were used to screen and filter the variants. The candidate was validated by Sanger sequencing. Conservation analysis and homology modelling were conducted.

Results: A heterozygous missense mutation c.1175C>T in the *PTCH1* gene predicting p.Ala392Val was identified. This variant has not been reported and was predicted to be deleterious. Sanger sequencing verified the variant and the dominant inheritance model in the family. The missense alteration affects an amino acid that is evolutionarily conserved in the first extracellular loop of the PTCH1 protein. The local structure of the mutant protein was significantly altered according to homology modelling.

Conclusions: Our findings suggest that c.1175C>T in *PTCH1* (NM_000264) may be the causative mutation of this pedigree. Our results add to the evidence that *PTCH1* variants play a role in the pathogenesis of orofacial clefts.

KEYWORDS
hereditary pedigree, nonsyndromic cleft lip and/or palate, *PTCH1*, whole exome sequencing

1 | INTRODUCTION

Cleft lip and/or palate (CL/P) is the most common craniofacial congenital abnormality, imposing substantial financial and health care burdens on the affected individuals, families and society (Mossey, Little, Munger, Dixon, & Shaw, 2009; Wehby & Cassell, 2010). CL/P affects generally 1/700 newborns worldwide, but this rate varies depending on geographic origin and racial/ethnic group (Dixon, Marazita, Beaty, & Murray, 2011). In general, the birth prevalence rates are reported to be highest in Asia, often as high as 1 in 500. CL/P-affected individuals may face problems such as feeding, speaking, hearing, malocclusion and mental health that necessitate a long-term multidisciplinary treatment approach, including surgery, orthodontic treatment, speech therapy, ear, nose and throat treatment, and psychosocial intervention.

*These authors contributed equally to this work.

CL/P can be divided into syndromic (SCL/P) (30%) and nonsyndromic (NSCL/P) forms (70%), depending on whether the affected patient has other systematic malformations. The aetiology of nonsyndromic CL/P is heterogeneous, involving a variety of interacting factors including genetic, environmental, geographic, ethnic and racial factors, as well as socioeconomic status (Grosen et al., 2010). About, most CL/P (70%) and cleft palate only (CPO) (50%) cases occur as isolated forms (FitzPatrick, Raine, & Boorman, 1994; Jones, 1988). Combining epidemiologic, genomewide studies, candidate gene, animal models and high-throughput sequencing has provided deeper insights into the aetiology of NSCL/P (Dixon et al., 2011).

Patched 1 (*PTCH1*), which is homologous to the *D. melanogaster* segment polarity gene, maps to 9q22.32. It consists of 23 coding exons and encodes an approximately 140 kDa transmembrane receptor, comprising 12 transmembrane domains, two extracellular loops (ECLs) and a putative sterol-sensing domain (SSD). It is involved in the Hedgehog (Hh) pathway, which is highly conserved among vertebrates. The pathway plays a pivotal role in embryonic body patterning and development (Briscoe & Therond, 2013). Dysfunction of this pathway can therefore result in various developmental defects. Numerous mutations of *PTCH1* have been identified in patients affected with Gorlin Syndrome, also termed basal cell naevus syndrome. Orofacial clefting is one of its clinical manifestations affecting 4%–9% of patients (Fujii & Miyashita, 2014; Kimonis et al., 2013). A recent genomewide association study (GWAS) in a Chinese population identified a marker at 9q22.32, located in an intronic region of *PTCH1* that has been associated with CL/P (Y. Yu et al., 2017). Mouse models defective in *Ptch1* showed craniofacial defects, including cleft lip, underdeveloped palatal shelves and clefting of the secondary palate (Feng, Choi, Clouthier, Niswander, & Williams, 2013; Kurosaka, Iulianella, Williams, & Trainor, 2014; Metzis et al., 2013).

In our study, whole exome sequencing (WES) was performed in a Han Chinese three-generation family with CL/P. A heterozygous missense mutation c.1175C>T (NM_000264) in the *PTCH1* gene predicting p.Ala392Val was identified. This variant is not reported in current databases, predicted to be deleterious by in silico tools. Sanger sequencing verified the variant and the dominant inheritance model in the family. The mutant amino acid locates in the first ECL domain of the protein (amino acids 122–436). Multiple sequence alignment revealed that the amino acid has been highly conserved through evolution. In addition, the local structure of the protein varies significantly between the wild-type (WT) and mutant proteins, indicating that this amino acid change may be harmful and potentially disrupts the interaction between Hh and PTCH1 proteins. These findings suggest that this novel variant is a potential causative mutation of CL/P.

2 | MATERIALS AND METHODS

2.1 | Human subjects

A Han Chinese family with CL/P of unknown aetiology was recruited from Peking University Hospital of Stomatology to participate in this study. We also recruited an independent cohort of 65 CL/P-unaffected subjects with Han Chinese ancestry to investigate the allele frequency. Ethical approval for the human subject study was obtained from the Human Research Ethics Committee of Peking University Hospital of Stomatology (PKUSSIRB-20150012). Understanding written informed consent was obtained from the study subjects themselves or from the guardians.

Clinical examinations and diagnoses were provided separately by two oral and maxillofacial surgeons. Patients also received a whole-body physical examination to confirm no other organ malformations or deformities. Detailed exposure histories of the mother of the proband during pregnancy were collected, including smoking, drinking, disease history, medicine and supplement intake, and exposure to radiation, poisons and chemicals. Unaffected family members were examined and the possibility of occluded submucous CL/P.

We collected 2–4 ml peripheral blood samples from each participant. Genomic DNA was extracted according to the manufacturer's instructions with the QIAamp DNA Blood Mini Kit (Qiagen, Hilden, Germany).

2.2 | Whole exome sequencing (WES)

DNA libraries with enrichment of exonic sequences were constructed from the human subjects. High-throughput sequencing of the libraries was performed, and raw sequencing read files were generated using the BGISEQ-500 platform (BGI Inc., Beijing, China) (Huang et al., 2017). Adapter sequences, low-quality sequences and undetected bases were excluded. The remaining reads were processed by variant calling against the human GRCh37/hg19 reference database using the Burrows-Wheeler Aligner software (Li & Durbin, 2010). Variant discovery analysis was performed using the Genome Analysis Toolkit (GATK) according to the guidelines provided (https://software.broadinstitute.org/gatk/). Repeat reads were removed using Picard Tools (http://broadinstitute.github.io/picard/). Local realignment and base quality recalibration were conducted using the GATK. Sequencing depth, target coverage and capture specificity were calculated based on the aligned data. In a subsequent way, single-nucleotide polymorphisms (SNPs) and insertions/deletions (InDels) were detected and filtered using HaplotypeCaller (GATK v3.3.0). SnpEff (http://snpeff.sourceforge.net/SnpEff_manual.html) was then used to perform annotation and prediction.

2.3 | Screening of variants

After annotation, we applied a filtration process to identify the candidate gene mutation. We included variants with a minor allele frequency (MAF) <0.05 in the 1,000 Genomes Project database (http://www.1000genomes.org/) and the ExAC Browser (http://exac.broadinstitute.org/). The mutation region was considered, and variants such as nonsynonymous variants, splice acceptor-site

or donor-site mutations, inserts and deletions were included. A Mendelian inheritance model was used to narrow down the candidates. In a subsequent way, we used in silico tools PolyPhen-2 (http://genetics.bwh.harvard.edu/pph2/) and SIFT (http://sift.jcvi.org/) to predict the potential functional effects of the variants and included variants that were predicted to be deleterious by either tool. At last, the literature was reviewed to identify the potential causative variant.

2.4 | Confirmation by Sanger sequencing

Considering the possibility that the *PTCH1* mutation is a new polymorphism in Han Chinese population which has not been reported in the database, we performed Sanger sequencing for validation on the family members and 65 unaffected subjects. PCR primers were designed (forward: 5′-ACAGATTCTATGCCTTGC-3′; reverse: 5′-TCCCCTTCCTGTTTCA-3′) using Primer Premier 5.0 and BLAST hosted by NCBI (https://blast.ncbi.nlm.nih.gov/Blast.cgi). The Sanger sequencing data were analysed using Chromas v1.0.0.1 software.

2.5 | Conservative analysis and homology model

Conservative analysis of the mutation position was conducted using UniProt (http://www.uniprot.org/) and ClustalX V2.1. To obtain more insight into the effects of the mutation on the molecular structure of PTCH1, a homology model was created using the online tool SWISS-MODEL (https://www.swissmodel.expasy.org/) (Biasini et al., 2014). Template 5u74.1 (Niemann-Pick C1 protein) was used to create the model for residues 46–436. PyMOL software was used for visualization.

3 | RESULTS

3.1 | Phenotypic descriptions of the pedigree

We recruited a three-generation Han Chinese family with isolated CL/P. There was no known consanguinity. The female proband (D1) presented with right complete CL/P, and her mother exhibited the same phenotype (D2) (Figure 1a,b). Both patients received a detailed general physical examination, including eyes and vision, external ear

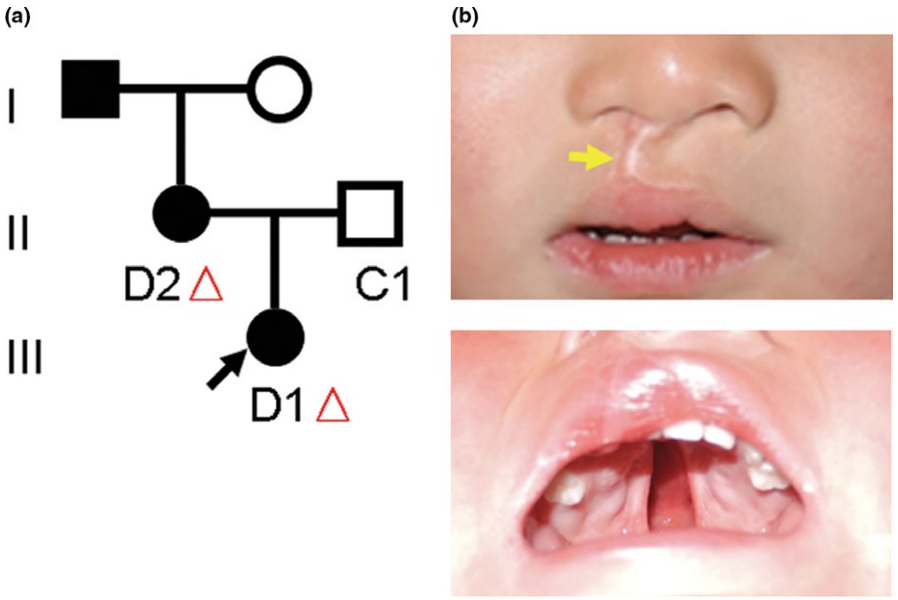

FIGURE 1 Pedigree and phenotypic information of a Han Chinese family with CL/P. (a) The proband (D1) is a female patient who exhibited right CL/P. Her mother, D2, exhibited the same phenotype. The father of D2 was also affected but was unavailable for examination. Filled symbols indicate the patients, whereas open symbols indicate unaffected members. Triangles indicate subjects who underwent WES. The black arrow indicates the proband. (b) Phenotype of D1. The yellow arrow indicates scars from right cleft lip repair

TABLE 1 Summary of whole exome sequencing data and alignment

Sample	Total effective yield (Gb)	Average sequencing depth	Q20%	Q30%	Mapping rate on genome (%)	Coverage of exome (%)	Target capture specificity (%)	Fraction of target covered≥4x (%)	Fraction of target covered≥20x (%)
D1	21.05	257.87	97.58	91.54	99.98	99.69	70.53	99.39	97.81
D2	29.45	249.21	97.10	90.42	99.95	99.77	48.73	99.52	97.56
Average	25.25	253.54	97.34	90.98	99.97	99.73	59.63	99.46	97.69

morphology and hearing, cranio-skeletal development, long bone morphology, neuromuscular and motor system function, cardiovascular system function and external genital system morphology, to eliminate the possibility of systemic malformation. Therefore, these two patients were diagnosed with NSCL/P. The father (C1) was non-dysmorphic. The grandfather from the maternal side was also affected by CL/P but was not available for examination.

During her pregnancy at age 25 years, D2 was exposed to passive smoking, although the frequency was low. There was no exposure to other factors, including diseases, alcohol, and radioactive or chemical teratogens, and no supplementation of folic acid, iron, vitamin B6 or antibiotics.

3.2 | A rare *PTCH1* mutation identified by WES and screening of variants

We performed WES on the two patients (D1 and D2) in this NSCL/P hereditary family. Each sample yielded 25.25 Gb data of mappable targeted exome sequences with a mean sequencing depth of greater than 250-fold. In total, 97.69% of the exonic regions were covered at least 20-fold (Table 1).

After mapping the sequences to the human GRCh37/hg19 reference genome, we identified 125,093 variants (including single and multiple nucleotide, insertion, and deletion variants) on average, of which 69,451 were heterozygous variants and 55,642 homozygous variants (Table 2). Both the quantity and quality of the sequencing met the requirements for further analysis.

After annotation of the variants, we applied a screening and filtration process to identify the candidate gene mutation (Figure 2a). Variants with MAF ≥ 0.05 in the 1,000 Genomes and ExAC databases were filtered out, leaving 18,040 variants. We then focused on variants that were more likely to be pathogenic, such as nonsynonymous variants, splice acceptor-site or donor-site mutations, and InDels, resulting in 2,180 variants. In a subsequent way, given that the family probably showed a dominant inheritance model, we selected heterozygous variants shared by D1 and D2, and 1,308 variants were found. We then used the bioinformatic tools PolyPhen-2 and SIFT to predict the potential functional effects. In total, 298 variants with moderate or high impact were predicted to be deleterious by either tool. Next, we examined previously reported genes with known roles in the pathogenesis of CL/P. We also sought information regarding some genes. At last, we identified c.1175C>T (NM_000264) in *PTCH1*, predicting p.Ala392Val, which results in a missense mutation that was assessed as deleterious, according to a Polyphen-2 score of 0.998 (the most deleterious Polyphen-2 score is 1.00).

3.3 | Verification of the *PTCH1* mutation by Sanger sequencing

The Sanger sequencing on the independent Han Chinese cohort (Table 3) did not detect any c.1175C>T variant (Supporting Information Appendix S1), excluding the possibility that the variant is

TABLE 2 Summary statistics for identified variants

Sample	Total variation	Heterozygotes	Homozygotes	Exonic	Intronic	Intergeneric	Splicing	Synonymous	Missense	Stop-gain	Stop-loss
D1	117,208	64,987	52,221	28,438	78,879	2,980	2,298	10,920	10,239	91	45
D2	132,978	73,914	59,064	29,433	92,667	3,107	2,302	11,029	10,391	94	45
Average	125,093	69,451	55,642	28,936	85,823	3,044	2,300	10,975	910,315	93	45

a novel SNP. We also validated the *PTCH1* mutation in both patients and the unaffected father (Figure 2b). Both patients were heterozygous for the mutant allele, while the father had the WT allele, which was in agreement with the WES results and the autosomal dominant inheritance pattern.

3.4 | Potential deleterious effects of the variant indicated by conservative analysis and modelling

The c.1175C>T_p.Ala392Val variant affects a highly conserved amino acid located in the first ECL domain of the PTCH1 protein (Figure 2c), suggesting that a genetic variant at this position is likely deleterious. Furthermore, the homology model for PTCH1 revealed a significant difference in the structures between the WT and mutant proteins (Figure 3). In the WT model, the residues mainly formed irregular coils (Phe376–Glu389) joined by a sheet (Glu389–Lys391). However, in the mutant simulation, the coils were denser, and the sheet structure was not apparent. Moreover, the C-terminal α-helix continued around the mutant position (Lys391–Ala393), which is different from the WT protein. The effect of the p.Ala392Val substitution on the local structure of the ECL may affect the protein's interaction with Hh within the biological complex.

4 | DISCUSSION

Multiple GWASs have identified susceptible loci that are significantly associated with CL/P in different populations (Beaty et al., 2010; Birnbaum et al., 2009; Grant et al., 2009; Leslie et al., 2016; Qian et al., 2016; Sun et al., 2015; Yu et al., 2017). However, GWAS has its own limitations. First, disease-causing variants occur in the healthy population at low frequencies, but a GWAS usually investigates variants with higher allele frequencies (usually >0.05) (Birnbaum et al., 2009). Therefore, it is difficult to determine the association between NSCL/P and those rare variants with lower allele frequencies (Vieira, 2008). Second, GWAS may bring about more false-positive and false-negative results because it mainly relies on statistical analyses. Moreover, GWAS identifies only the association between the risk locus and the

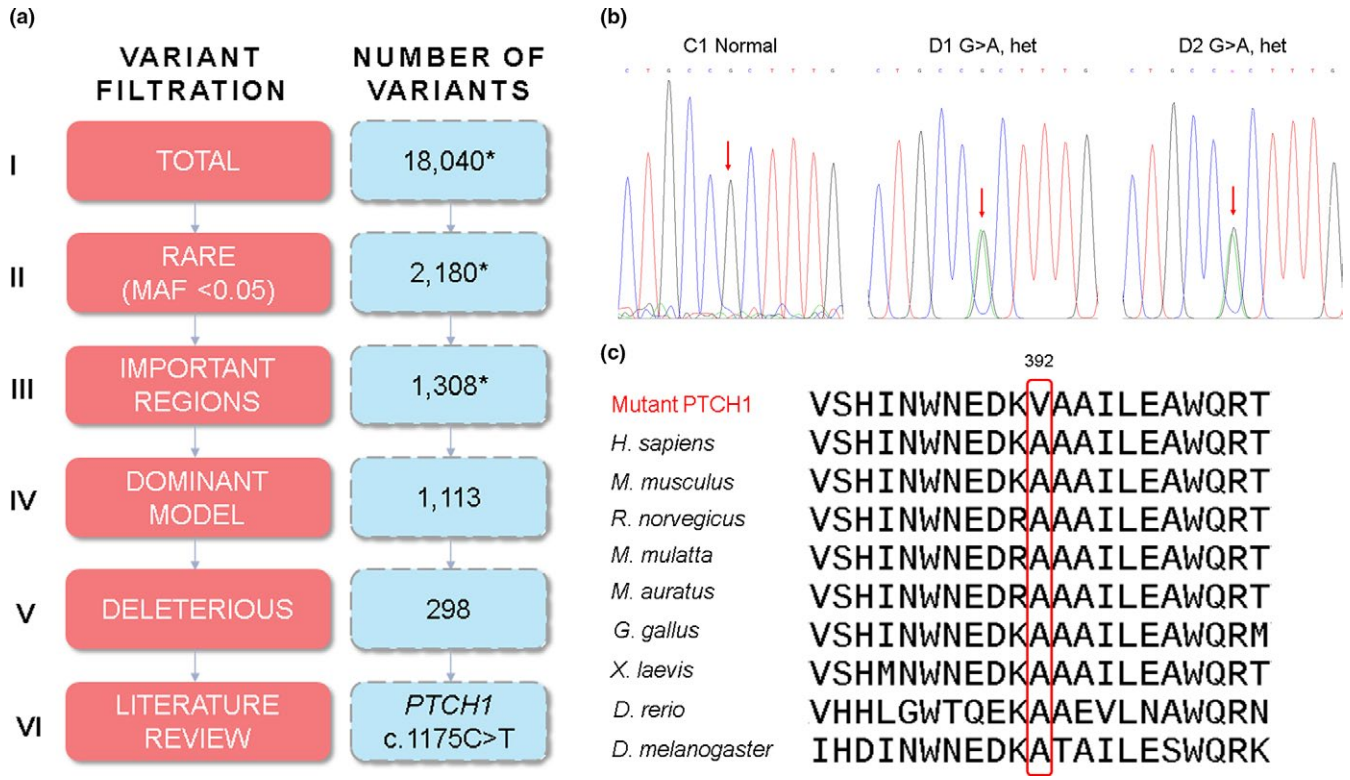

FIGURE 2 (a) Causative gene mutation filtration of the three-generation NSCL/P pedigree. Numbers marked with * indicate averaged variants between D1 and D2. (b) Sanger sequencing validation of the *PTCH1* c.1175C>T mutation, shown as the reverse complementary sequence. C1 was found to have the WT protein, while D1 and D2 carried the same heterozygous G>A mutation. Red arrows indicate the position of the *PTCH1* mutation. (c) Multiple sequence alignment showing evolutionary conservation of the PTCH1 residue Ala392 affected by the variant. The amino acid is highly conserved among vertebrates as well as *D. melanogaster*

TABLE 3 Allele frequencies in various population reported in databases and our Han Chinese cohort

1,000 genomes all	1,000 genomes Asian populations	1,000 genomes European populations	1,000 genomes African populations	ExAC	Our cohort of 65 unaffected Han Chinese subjects
0	0	0	0	0	0

disease, rather than the actual causal relationship, making it difficult to interpret the underlying mechanisms of phenotype occurrence. In recent years, next-generation sequencing, including whole-genome and WES, has been used to determine causal variation and interpret the aetiologic mechanisms of the NSCL/P hereditary pedigree (Tian et al., 2017; Wu et al., 2015). These techniques complement GWASs and together cover the spectrum of NSCL/P mutations.

In this study, we performed WES in an affected mother and her daughter with right CL/P from a Han Chinese family. After narrowing down the detected variants using a Mendelian inheritance model, public databases, in silico prediction tools and a literature review, we identified a novel missense mutation in the *PTCH1* gene: c.1175C>T predicting p.Ala392Val. This variant was confirmed by Sanger sequencing. Conservative analysis and homology models indicated that this variant may alter the normal structure and function of the protein and is therefore a potential cause of the phenotype.

As a genetically complex disease, NSCL/P may have multiple genetic models, including dominant (Birnbaum et al., 2008; Holzinger et al., 2017; Tian et al., 2017) and recessive inheritance (Marazita et al., 2004; Moura, Cirio, & Pimpao, 2012). Based on the family pedigree information in this study, an autosomal dominant Mendelian inheritance model was considered the best fit, although we cannot eliminate the possibility of de novo, homozygous, or compound heterozygous models.

Our study identified a missense mutation in the *PTCH1* coding sequence of the affected mother and daughter, which was predicted to be probably damaging to PTCH1 protein function. Consistent with this, multiple sequence alignment revealed the mutation occurred at an amino acid that was highly conserved. PTCH1 acts as the receptor of Hedgehog (Hh), a secreted molecule participated in the embryonic structures formation. It encodes a 1447-amino acid transmembrane protein. Mutations of *PTCH1* have been shown previously to play a crucial role in the aetiology of Gorlin Syndrome, a rare autosomal dominant disorder (Guo et al., 2013; Klein, Dykas, & Bale, 2005). Gorlin syndrome patients are characterized by basal cell carcinomas development since an early age. Also, other characteristic facial features, for example, cleft lip and/or palate, frontal bossing and macrocephaly present in a significant proportion of affected individuals (Fujii & Miyashita, 2014). Mutations in *PTCH1* that result in the loss of function, such as insertions, deletions, missense and nonsense mutations (Klein et al., 2005), are found to occur in approximately 70% of patients affected with the syndrome (Smith et al., 2014).

Three *PTCH1* missense variants were also identified in a sequence screening of NSCL/P patients (Mansilla et al., 2006). In addition, an SNP (rs10512248) located in the introgenic region of *PTCH1* was found to be associated with NSCL/P (p = 5.10E−10) (Yu et al., 2017).

Evidence from animal models has demonstrated that disrupting *Ptch1* function results in CL/P pathogenesis. A decrease in the

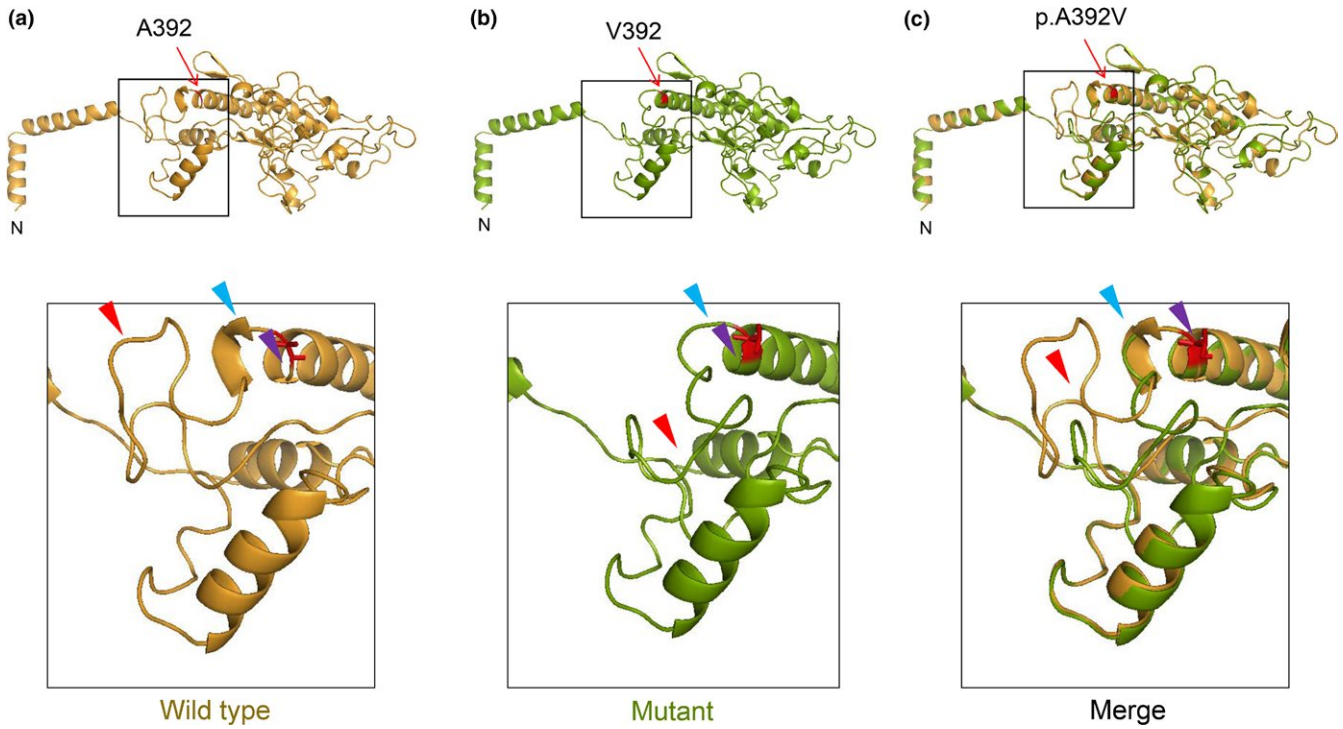

FIGURE 3 Homology model for the (a) WT (yellow) and (b) mutant (green) PTCH1 residues 46–436. (c) Merged view. *Upper panel:* the mutated position is depicted in red and indicated by a red arrow. Framed regions are magnified in the *lower panel*: the substitution p.Ala392Val has a strong influence on the structure compared with the WT protein, which is indicated by three arrowheads. Red: residues Phe376–Glu389 form two loose U-shaped structures in the WT protein, whereas in the mutant protein model, the region (Met367–Asn388) changes to a loose L-shaped structure. Blue: a sheet in the region of Glu389–Lys391 in the WT protein is replaced by a loose structure in the mutant protein. Purple: in the mutant protein model, residues Lys391–Ala393 continue to form the α-helix, whereas this region is a coil in the WT protein model

Drosophila segment polarity gene Patched, a homolog of human PTCH1, was found to lead to the developmental malformations observed in Gorlin syndrome (Hahn et al., 1996). Deletion of *Ptch1* in the facial mesenchyme influences cell morphology, resulting in cleft lip phenotype (Kurosaka et al., 2014; Metzis et al., 2013). *Ptch1*^{DL}-defective mice present underdeveloped palatal shelves and clefting of the secondary palate (Feng et al., 2013).

PTCH1 protein consists of several crucial functional domains, including two ECLs, one putative SSD, one large intracellular loop and 12 transmembrane regions. The ECLs are the binding sites of Hh protein to the PTCH1 protein (Marigo, Davey, Zuo, Cunningham, & Tabin, 1996). The SSD, which harbours transmembrane domains 2–6, may suppress Smoothened activity (Martin, Carrillo, Torroja, & Guerrero, 2001; Strutt et al., 2001). Taken together, Hh binding to PTCH1 inhibits the degradation of Smoothened (Zhao, Tong, & Jiang, 2007). This depression subsequently results in activation of the Gli family, the only transcriptional factors of the Hh signalling pathway that has been reported (Hui & Angers, 2011). Regulating the nuclear translocation of Gli proteins is a crucial step in the Hh signalling cascade. In addition, the ICL domain regulates the subcellular localization of M-phase promoting factor, implicating in the G2/M checkpoint of cell mitosis, which suggests a role of PTCH1 in the regulation of cell division (Yu, You, Yan, & Chen, 2014).

The variant p.Ala392Val identified in this study is located in the first ECL domain of PTCH1, which was found to be one of the *PTCH1* mutation hotspots (nearly 30%) in Gorlin syndrome (Guo et al., 2013). According to our molecular modelling results, residues 376–393 of the ECL structure may be significantly altered. Given that the variant was predicted to be deleterious, the function of the ECL domain may be disrupted, which would subsequently influence the Hh signalling pathway and ultimately result in the described phenotypes.

However, this was a preliminary discovery of the causative mutation for the CL/P-affected family. The pathogenic mechanisms of *PTCH1* mutations that cause orofacial clefts are not fully understood and require further demonstration in animal models and cellular/molecular experiments.

In conclusion, we found a novel single-nucleotide mutation in the coding region of *PTCH1* by WES in a NSCL/P hereditary pedigree. Preliminary studies such as functional prediction, conservation analysis and homology modelling suggested that the variant c.1175C>T_p.Ala392Val potentially underlies CL/P in this pedigree. Our data further add to the increasing evidence that *PTCH1* variants underlie in the aetiology of nonsyndromic orofacial clefts.

ACKNOWLEDGEMENTS

The Beijing Municipal Natural Science Foundation (No. 7182184) and Interdisciplinary Medicine Seed Fund of Peking University (No. BMU2017 MB006).

CONFLICT OF INTERESTS

None to declare.

AUTHOR CONTRIBUTION

H. Zhao and W. Zhong analysed data, conducted PCR and drafted the paper. C. Leng examined the affected patients. J. Zhang collected human subjects and analyzed data. M. Zhang, W. Huang and Y. Zhang analyzed data. W. Li, P. Jia and J. Lin collected human subjects. Gulibaha Maimaitili and Feng Chen designed the study.

ORCID

Feng Chen http://orcid.org/0000-0003-3041-9569

REFERENCES

Beaty, T. H., Murray, J. C., Marazita, M. L., Munger, R. G., Ruczinski, I., Hetmanski, J. B., … Scott, A. F. (2010). A genome-wide association study of cleft lip with and without cleft palate identifies risk variants near MAFB and ABCA4. *Nature Genetics*, *42*(6), 525–529. https://doi.org/10.1038/ng.580

Biasini, M., Bienert, S., Waterhouse, A., Arnold, K., Studer, G., Schmidt, T., … Schwede, T. (2014). SWISS-MODEL: Modelling protein tertiary and quaternary structure using evolutionary information. *Nucleic Acids Research*, *42*, W252–W258. https://doi.org/10.1093/nar/gku340(Web Server issue)

Birnbaum, S., Ludwig, K. U., Reutter, H., Herms, S., Steffens, M., Rubini, M., … Mangold, E. (2009). Key susceptibility locus for nonsyndromic cleft lip with or without cleft palate on chromosome 8q24. *Nature Genetics*, *41*(4), 473–477. https://doi.org/10.1038/ng.333

Birnbaum, S., Reutter, H., Lauster, C., Scheer, M., Schmidt, G., Saffar, M., … Mangold, E. (2008). Mutation screening in the IRF6-gene in patients with apparently nonsyndromic orofacial clefts and a positive family history suggestive of autosomal-dominant inheritance. *American Journal of Medical Genetics Part A*, *146a*(6), 787–790. https://doi.org/10.1002/ajmg.a.32219

Briscoe, J., & Therond, P. P. (2013). The mechanisms of Hedgehog signalling and its roles in development and disease. *Nature Reviews Molecular Cell Biology*, *14*(7), 416–429. https://doi.org/10.1038/nrm3598

Dixon, M. J., Marazita, M. L., Beaty, T. H., & Murray, J. C. (2011). Cleft lip and palate: Understanding genetic and environmental influences. *Nature Reviews Genetics*, *12*(3), 167–178. https://doi.org/10.1038/nrg2933

Feng, W., Choi, I., Clouthier, D. E., Niswander, L., & Williams, T. (2013). The *Ptch1*(DL) mouse: A new model to study lambdoid craniosynostosis and basal cell nevus syndrome-associated skeletal defects. *Genesis (New York, N.Y.:2000)*, *51*(10), 677–689. https://doi.org/10.1002/dvg.22416

FitzPatrick, D. R., Raine, P. A., & Boorman, J. G. (1994). Facial clefts in the west of Scotland in the period 1980-1984: Epidemiology and genetic diagnoses. *Journal of Medical Genetics*, *31*(2), 126–129. https://doi.org/10.1136/jmg.31.2.126

Fujii, K., & Miyashita, T. (2014). Gorlin syndrome (nevoid basal cell carcinoma syndrome): Update and literature review. *Pediatrics International*, *56*(5), 667–674. https://doi.org/10.1111/ped.12461

Grant, S. F., Wang, K., Zhang, H., Glaberson, W., Annaiah, K., Kim, C. E., … Hakonarson, H. (2009). A genome-wide association study identifies a locus for nonsyndromic cleft lip with or without cleft palate on 8q24. *Journal of Pediatrics*, *155*(6), 909–913. https://doi.org/10.1016/j.jpeds.2009.06.020

Grosen, D., Chevrier, C., Skytthe, A., Bille, C., Molsted, K., Sivertsen, A., … Christensen, K. (2010). A cohort study of recurrence patterns among more than 54,000 relatives of oral cleft cases in Denmark:

Support for the multifactorial threshold model of inheritance. *Journal of Medical Genetics*, *47*(3), 162–168. https://doi.org/10.1136/jmg.2009.069385

Guo, Y. Y., Zhang, J. Y., Li, X. F., Luo, H. Y., Chen, F., & Li, T. J. (2013). *PTCH1* gene mutations in Keratocystic odontogenic tumors: A study of 43 Chinese patients and a systematic review. *PLoS One*, *8*(10), e77305. https://doi.org/10.1371/journal.pone.0077305

Hahn, H., Wicking, C., Zaphiropoulous, P. G., Gailani, M. R., Shanley, S., Chidambaram, A., … Bale, A. E. (1996). Mutations of the human homolog of Drosophila patched in the nevoid basal cell carcinoma syndrome. *Cell*, *85*(6), 841–851. https://doi.org/10.1016/S0092-8674(00)81268-4

Holzinger, E. R., Li, Q., Parker, M. M., Hetmanski, J. B., Marazita, M. L., Mangold, E., … Bailey-Wilson, J. E. (2017). Analysis of sequence data to identify potential risk variants for oral clefts in multiplex families. *Molecular Genetics & Genomic Medicine*, *5*(5), 570–579. https://doi.org/10.1002/mgg3.320

Huang, J., Liang, X., Xuan, Y., Geng, C., Li, Y., Lu, H., … Gao, S. (2017). A reference human genome dataset of the BGISEQ-500 sequencer. *Gigascience*, *6*(5), 1–9. https://doi.org/10.1093/gigascience/gix024

Hui, C. C., & Angers, S. (2011). Gli proteins in development and disease. *Annual Review of Cell and Developmental Biology*, *27*, 513–537. https://doi.org/10.1146/annurev-cellbio-092910-154048

Jones, M. C. (1988). Etiology of facial clefts: Prospective evaluation of 428 patients. *The Cleft Palate Journal*, *25*(1), 16–20.

Kimonis, V. E., Singh, K. E., Zhong, R., Pastakia, B., Digiovanna, J. J., & Bale, S. J. (2013). Clinical and radiological features in young individuals with nevoid basal cell carcinoma syndrome. *Genetics in Medicine*, *15*(1), 79–83. https://doi.org/10.1038/gim.2012.96

Klein, R. D., Dykas, D. J., & Bale, A. E. (2005). Clinical testing for the nevoid basal cell carcinoma syndrome in a DNA diagnostic laboratory. *Genetics in Medicine*, *7*(9), 611–619. https://doi.org/10.109701.gim.0000182879.57182.b4

Kurosaka, H., Iulianella, A., Williams, T., & Trainor, P. A. (2014). Disrupting hedgehog and WNT signaling interactions promotes cleft lip pathogenesis. *Journal of Clinical Investigation*, *124*(4), 1660–1671. https://doi.org/10.1172/jci72688

Leslie, E. J., Liu, H., Carlson, J. C., Shaffer, J. R., Feingold, E., Wehby, G., … Marazita, M. L. (2016). A Genome-wide Association Study of Nonsyndromic Cleft Palate Identifies an Etiologic Missense Variant in GRHL3. *American Journal of Human Genetics*, *98*(4), 744–754. https://doi.org/10.1016/j.ajhg.2016.02.014

Li, H., & Durbin, R. (2010). Fast and accurate long-read alignment with Burrows-Wheeler transform. *Bioinformatics*, *26*(5), 589–595. https://doi.org/10.1093/bioinformatics/btp698

Mansilla, M. A., Cooper, M. E., Goldstein, T., Castilla, E. E., Lopez Camelo, J. S., Marazita, M. L., & Murray, J. C. (2006). Contributions of PTCH gene variants to isolated cleft lip and palate. *Cleft Palate-Craniofacial Journal*, *43*(1), 21–29. https://doi.org/10.1597/04-169r.1

Marazita, M. L., Field, L. L., Tuncbilek, G., Cooper, M. E., Goldstein, T., & Gursu, K. G. (2004). Genome-scan for loci involved in cleft lip with or without cleft palate in consanguineous families from Turkey. *American Journal of Medical Genetics Part A*, *126a*(2), 111–122. https://doi.org/10.1002/ajmg.a.20564

Marigo, V., Davey, R. A., Zuo, Y., Cunningham, J. M., & Tabin, C. J. (1996). Biochemical evidence that patched is the Hedgehog receptor. *Nature*, *384*(6605), 176–179. https://doi.org/10.1038/384176a0

Martin, V., Carrillo, G., Torroja, C., & Guerrero, I. (2001). The sterol-sensing domain of Patched protein seems to control Smoothened activity through Patched vesicular trafficking. *Current Biology*, *11*(8), 601–607. https://doi.org/10.1016/S0960-9822(01)00178-6

Metzis, V., Courtney, A. D., Kerr, M. C., Ferguson, C., Rondon Galeano, M. C., Parton, R. G., … Wicking, C. (2013). Patched1 is required in neural crest cells for the prevention of orofacial clefts. *Human Molecular Genetics*, *22*(24), 5026–5035. https://doi.org/10.1093/hmg/ddt353

Mossey, P. A., Little, J., Munger, R. G., Dixon, M. J., & Shaw, W. C. (2009). Cleft lip and palate. *Lancet*, *374*(9703), 1773–1785. https://doi.org/10.1016/s0140-6736(09)60695-4

Moura, E., Cirio, S. M., & Pimpao, C. T. (2012). Nonsyndromic cleft lip and palate in boxer dogs: Evidence of monogenic autosomal recessive inheritance. *Cleft Palate-Craniofacial Journal*, *49*(6), 759–760. https://doi.org/10.1597/11-110

Qian, Y., Li, D., Ma, L., Zhang, H., Gong, M., Li, S., … Wang, L. (2016). TPM1 polymorphisms and nonsyndromic orofacial clefts susceptibility in a Chinese Han population. *American Journal of Medical Genetics Part A*, *170a*(5), 1208–1215. https://doi.org/10.1002/ajmg.a.37561

Smith, M. J., Beetz, C., Williams, S. G., Bhaskar, S. S., O'Sullivan, J., Anderson, B., … Evans, D. G. (2014). Germline mutations in SUFU cause Gorlin syndrome-associated childhood medulloblastoma and redefine the risk associated with *PTCH1* mutations. *Journal of Clinical Oncology*, *32*(36), 4155–4161. https://doi.org/10.1200/jco.2014.58.2569

Strutt, H., Thomas, C., Nakano, Y., Stark, D., Neave, B., Taylor, A. M., & Ingham, P. W. (2001). Mutations in the sterol-sensing domain of Patched suggest a role for vesicular trafficking in Smoothened regulation. *Current Biology*, *11*(8), 608–613. https://doi.org/10.1016/S0960-9822(01)00179-8

Sun, Y., Huang, Y., Yin, A., Pan, Y., Wang, Y., Wang, C., … Yang, Y. (2015). Genome-wide association study identifies a new susceptibility locus for cleft lip with or without a cleft palate. *Nature Communications*, *6*, 6414. https://doi.org/10.1038/ncomms7414

Tian, H., Feng, J., Li, J., Ho, T. V., Yuan, Y., Liu, Y., … Chai, Y. (2017). Intraflagellar transport 88 (IFT88) is crucial for craniofacial development in mice and is a candidate gene for human cleft lip and palate. *Human Molecular Genetics*, *26*(5), 860–872. https://doi.org/10.1093/hmg/ddx002

Vieira, A. R. (2008). Unraveling human cleft lip and palate research. *Journal of Dental Research*, *87*(2), 119–125. https://doi.org/10.1177/154405910808700202

Wehby, G. L., & Cassell, C. H. (2010). The impact of orofacial clefts on quality of life and healthcare use and costs. *Oral Diseases*, *16*(1), 3–10. https://doi.org/10.1111/j.1601-0825.2009.01588.x

Wu, D., Mandal, S., Choi, A., Anderson, A., Prochazkova, M., Perry, H., … Slavotinek, A. M. (2015). DLX4 is associated with orofacial clefting and abnormal jaw development. *Human Molecular Genetics*, *24*(15), 4340–4352. https://doi.org/10.1093/hmg/ddv167

Yu, Y. R., You, L. R., Yan, Y. T., & Chen, C. M. (2014). Role of OVCA1/DPH1 in craniofacial abnormalities of Miller-Dieker syndrome. *Human Molecular Genetics*, *23*(21), 5579–5596. https://doi.org/10.1093/hmg/ddu273

Yu, Y., Zuo, X., He, M., Gao, J., Fu, Y., Qin, C., … Bian, Z. (2017). Genome-wide analyses of non-syndromic cleft lip with palate identify 14 novel loci and genetic heterogeneity. *Nature Communications*, *8*, 14364. https://doi.org/10.1038/ncomms14364

Zhao, Y., Tong, C., & Jiang, J. (2007). Hedgehog regulates smoothened activity by inducing a conformational switch. *Nature*, *450*(7167), 252–258. https://doi.org/10.1038/nature06225

SUPPORTING INFORMATION

Additional supporting information may be found online in the Supporting Information section at the end of the article.

How to cite this article: Zhao H, Zhong W, Leng C, et al. A novel *PTCH1* mutation underlies nonsyndromic cleft lip and/or palate in a Han Chinese family. *Oral Dis*. 2018;24:1318–1325. https://doi.org/10.1111/odi.12915